Applied Energy 206 (2017) 267–277

Contents lists available at ScienceDirect

Applied Energy

journal homepage: www.elsevier.com/locate/apenergy

Electricity demand planning forecasts should consider climate non-stationarity to maintain reserve margins during heat waves

Daniel Burillo[a,*], Mikhail V. Chester[a], Benjamin Ruddell[b], Nathan Johnson[c]

[a] Civil, Environmental and Sustainable Engineering, Arizona State University, USA
[b] School of Informatics, Computing, and Cyber Systems, Northern Arizona University, USA
[c] The Polytechnic School, Ira A. Fulton Schools of Engineering, Arizona State University, USA

HIGHLIGHTS

- Weather-adjustment methods in electricity infrastructure planning are biased.
- Climate models project temperatures up to 58 °C (136 °F) in the US Desert Southwest.
- Peak demand does not increase linearly with temperature; s-curve more accurate.
- Los Angeles could experience hazardous power shortages in record-breaking heat.
- Risk management strategies identified via reductions in peak load & load variance.

ARTICLE INFO

Keywords:
Climate non-stationarity
Electric power infrastructure
Peak demand
Risk management
Structural equation modeling

ABSTRACT

Climate non-stationarity is a challenge for electric power infrastructure reliability; recordbreaking heat waves significantly affect peak demand [1], lower contingency capacities, and expose cities to risk of blackouts due to component failures and security threats. The United States' electric grid operates safely for a wide range of load, weather, and power quality conditions. Projected increases in ambient air temperatures could, however, create operating conditions that place the grid outside the boundaries of current reliability tolerances. Advancements in long-term forecasting, including projections of rising air temperatures and more severe heat waves, present opportunities to advance risk management methods for long-term infrastructure planning. This is particularly evident in the US Southwest—a relatively hot region expected to experience significant temperature increases affecting electric loads, generation, and delivery systems. Generation capacity is typically built to meet the 90th percentile (*T90*) hottest peak demand, plus an additional reserve margin of least 15%, but that may not be sufficient to ensure reliable power services if air temperatures are higher than expected. The problem with this *T90* planning approach is that it requires a stationary climate to be completely effective. In reality, annual temperature differences can have more than a 15% effect on system performance. Current long-term infrastructure planning and risk management processes are biased climate data choices that can significantly underestimate peak demand, overestimate generation capacity, and result in major power outages during heat waves.

This study used downscaled global climate models (GCMs) to evaluate the effects of non-stationarity on air temperature forecasts, and a new high-level statistical approach was developed to consider the subsequent effects on peak demand, power generation, and local reserve margins (LRMs) compared to previous forecasting methods. Air temperature projections in IPCC RCPs 4.5 and 8.5 are that increases up to 6 °C are possible by the end of century, with highs of 58 °C and 56 °C in Phoenix, Arizona and Los Angeles, California respectively. In the hottest scenarios, we estimated that LRMs for the two metro regions would be on average 30% less than at respective *T90*s, which in the case of Los Angeles (a net importer) would require 5 GW of additional power to meet electrical demand. We calculated these values by creating a structural equation model (SEM) for peak demand based on the physics of common AC units; physics-based models are necessary to predict demand under unprecedented conditions for which historical data do not exist. The SEM forecasts for peak demand were close to straight-line regression methods as in prior literature from 25–40 °C (104 °F), but diverged lower at higher temperatures. Power plant generation capacity derating factors were also modeled based on the electrical and thermal performance characteristics of different technologies. Lastly, we discussed several strategic options to

* Corresponding author.
E-mail addresses: Daniel.Burillo@asu.edu (D. Burillo), mchester@asu.edu (M.V. Chester), Benjamin.Ruddell@nau.edu (B. Ruddell), NathanJohnson@asu.edu (N. Johnson).

http://dx.doi.org/10.1016/j.apenergy.2017.08.141
Received 17 March 2017; Received in revised form 29 June 2017; Accepted 12 August 2017
0306-2619/

reduce the risk of LRM shortages; including implementing technology, market incentives, and urban forms that reduce peak load and load variance per capita as well as their tradeoffs with several other stakeholder objectives.

1. Introduction climate stationarity assumptions in long-term electricity infrastructure planning

Some risk management practices in the electric power sector use "rules of thumb." One of these rules is to build at least a 15% surplus of power generation to meet peak demand [2], where contingency capacity or generation "head room" is needed if units go offline. Maintaining a reliable margin is risky business because peak demand changes over time as a result of variations in population, human behavior, technology, and climate [3]; moreover, infrastructure implementations are costly and long-term investments. The electric power industry currently considers all of these factors in planning processes; however, they do not plan for climate non-stationarity [4–7]. Climate non-stationarity affects planning in two ways, wherein changing atmospheric conditions can result in different annual probability distributions of air temperatures [8], as well as differences in low, average, and high air temperatures [9]. The common practice in industry is to plan for future peak demand based on a 90th percentile, also referred to as *T90* or 1-in-10 hottest days, summertime temperature using historical (stationary) probability distributions [6,10]. Peak demand is generally understood to change with temperature during the seasons in many geographic regions, but little knowledge exists in environmental studies to model that relationship beyond historical correlations [11–16]. With a lack of peer-reviewed literature on the topic, studies can easily, and mistakenly, assume correlation implies causation when assessing the risk of rising air temperatures on infrastructure systems. Accurate scientific knowledge is necessary to maintain reliability in electric infrastructure systems if climate conditions are significantly different in the future.

Failure to properly understand and plan for grid performance at unprecedented high temperatures could result in blackouts. Multiple service interruptions have recently occurred during heat waves due to transformer overloads, transmission line faults, generation shortages, and cascading failures [17–20]. While grid operators can ramp power generators up or down to respond to sub hourly changes in load [21], those capabilities are physically limited by plant type, total production capacity, and bottlenecks in electrical delivery systems–all of which are determined through long-term planning processes [3]. If the forecasting methods are not accurate, and engineering tolerances are not sufficient, then contingency capacities could be negatively impacted and component hardware failures could be triggered; systems could be exposed to security threats [22,23], higher probability of blackouts [24], and unnecessary operations costs [3].

Local reserve margin (LRM) is a contingency capacity metric equal to the amount of generation that exceeds the aggregate peak demand within a geographic area. The "local" boundary can be a neighborhood, a substation region, a utility service territory, or several territories, and may or may not include "remote" generation and "long-distance" transmission lines [6,25–31]. Transmission import capabilities are out of the scope of local generation, and are dependent upon generation headroom in other connected local areas. These imports allow for a reduction in LRM regulatory requirements by enabling delivery of non-local resources [32]. Specific requirements for LRMs vary regionally with consideration for factors such as the reliability of components, likelihood of concurrent peak loads in neighboring regions, and security [25–27,33].

In this study, we examined assumptions about air temperatures used in long-term infrastructure planning processes, including the lack of consideration for annual differences in heat wave severity (non-stationarity), and corresponding methods for forecasting peak demand, generation capacity, and LRMs, which could result in power shortages. We used county lines for Los Angeles and Maricopa (Phoenix) to define local areas for LRMs because these geopolitical boundaries reasonably frame the existing infrastructure, and public data were readily accessible in that format. We used global climate model (GCM) simulations of the Intergovernmental Panel on Climate Change's Representative Carbon Pathway scenarios RCP 4.5 and RCP 8.5 to define a range of possible future air temperatures in addition to historical ranges from local weather stations. We modeled how existing infrastructure operates differently across the range of historical and future air temperatures using previous statistical methods from the literature and our own structural equation modeling approach. We did not attempt to predict physical changes in future supply- or demand-side infrastructure or complete a full planning scenario necessary for legislating local resource adequacy and transfer capacity requirements. Specifically, we studied the effects of stationarity assumptions on long-term planning estimates of (1) air temperatures, (2) peak demand, (3) generation capacity, and (4) LRM. We used our quantitative models and results as the premise for a qualitative discussion of options to mitigate the risk of LRM shortages.

2. Methods: Air temperature effects on peak demand, generation capacity, and LRMs

We chose the Phoenix and Los Angeles regions to study because they are the two largest cities in the US Southwest and have growing populations and aging infrastructure that require immediate investments [5,34,35]. These regions are already amongst the hottest in the world, are expected to have significant temperature increases in the future [1,11], and were feasible to study because they exist largely within county boundaries for which public data are available. First, we characterized ranges of local temperatures within and across Los Angeles, California and Maricopa, Arizona for recent historical samples of *T90* and GCM projections of future high temperatures for RCP 4.5 and RCP 8.5. Second, we fit two statistical models to historical data to predict peak demand as a function of air temperature. We used a straight-line regression approach, as in previous studies, and developed our own model based on AC performance at varying T_{max}. The nature of our model is that it has multiple levels of equations with terms that fit simultaneously as both predicted and predictor variables; this type of multiple regression analysis is called structural equation modeling (SEM) [36]. As explained in detail in SI Section 1, we chose to focus the majority of our analytical efforts on modeling peak demand because seasonal changes in peak demand are an order of magnitude higher than changes in generation capacity, which are an order of magnitude higher than any delivery system losses. We did not consider losses in any form. Third, we used derating factors from previous studies of power plant operations to estimate decreases in capacity as a function of T_{max} by generator fuel technology. Fourth and finally, we used results of those analyses to calculate LRM, and analyzed the effects of stationarity assumptions in the above aspects of LRM planning.

2.1. Local air temperatures

We parameterized a range of daily high air temperatures (T_{max}) using historical weather station data obtained from [37], and future projections from downscaled Localized Constructed Analogs GCM models through the end of century [38]. To quantify a range of temperature values for the stationarity approach, we sampled T_{max} from June, July, August, and September during the early-century period (2001–2016) from four weather stations in each county located where coincident power demand data were available in [11,12]. Fig. 1a shows the weather station locations geographically, and T_{max} for the historical period at 2 km x 2 km resolution. Data used for the map images were obtained from different sources due to technical reasons, and were used only to produce those map images [39–41]. The 90th percentile T_{max} values, *T90s*, shown in Fig. 1b, are the range of annual *T90s* from the lowest to highest years in the sample. The early T_{max} values represent the range of annual T_{max} values for the early-century period. For the non-stationary approach, we used mid-century (2041–2060) and late-century (2060–2099) LOCA T_{max} projections from the 32 GCMs available for RCP 4.5 and 8.5. GCM projections were obtained at $^1/_8{}^\circ \times {}^1/_8{}^\circ$ resolution for the locations indicated in Fig. 1a from [38], as these were the most comprehensive spatially detailed future forecasts publically available at the time. The highest T_{max} in each period for each GCM projection was sampled; the highest temperature in each period from each GCM, a.k.a. the "block maximum" [42] range for each of the 32 models was plotted side-by-side to the historical statistics in Fig. 1b to compare the differences in the ranges of uncertainties.

2.2. Peak demand

2.2.1. Electricity data

The sample of electricity data consisted of the daily maximum demand, which we extracted from the hourly time series values listed in EIA's US Electricity System Operating Data, Form 930 [43]. We collected peak demand data for three representative balancing authorities (LDWP – Los Angeles Department of Water and Power, AZPS – Arizona Public Service Company, and SRP – Salt River Project). The sampling period ranged from July 01, 2015 to September 15, 2016. Hourly load data were also obtained from Southern California Edison (SCE) [44], but were not used in the analysis because we were unable to reconcile differences between SCE's reported hourly (normalization-masked) loads and EIA's total annual demand values. Complete plots of peak demand observations are included in SI Section 5 for the best-fit

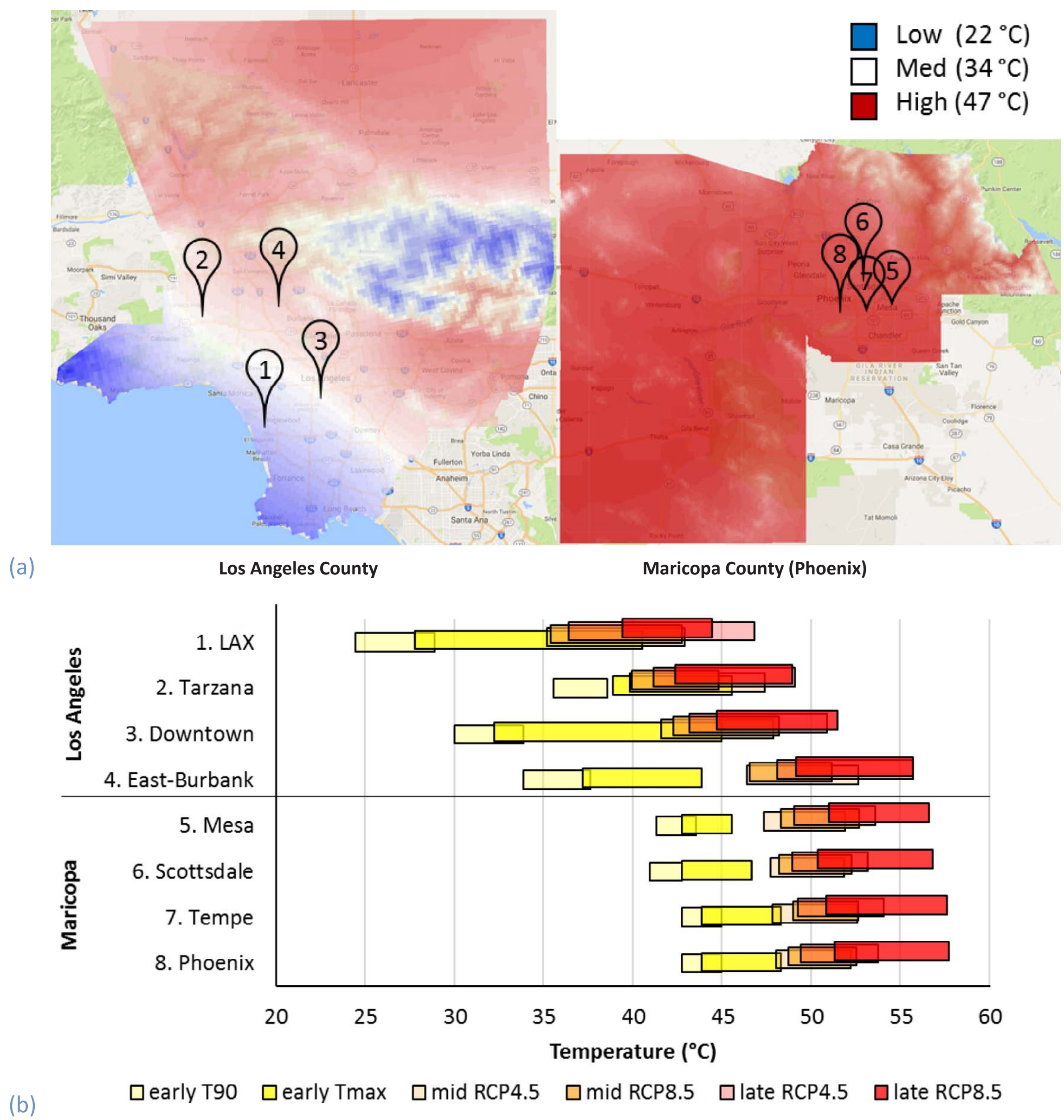

Fig. 1. (a) Map of county weather stations and early-century T_{max}. The Los Angeles locations 1–4 represent coastal, suburban, downtown, and desert landscapes respectively. The Phoenix locations 5–8 represent fringe suburb, two populous neighboring suburbs, and the urban heat island center respectively. (b) Comparison of local temperatures for early-, mid-, and late-century periods. Early-century (2001–2016) temperature ranges include annual *T90* and T_{max}. Mid-century (2041–2060) and late-century (2061–2099) ranges include the block maxima of the 32 GCMs sampled for each period and RCP.

balancing authority to weather station models. The number of observations was approximately 300 for each balancing authority and corresponding weather station at $T_{max} \geq 25$ °C (77 °F), which corresponds to most residential air conditioning (AC) thermostat settings in our sample regions [45,46]. The top T_{max} observations were 48 °C and 46 °C (118 °F and 115 °F) for Phoenix and Los Angeles respectively in the period [37]. Because the source data were based on measurements from balancing authority interconnections, they did not explicitly account for distributed energy resources or any delivery system losses. We considered adjusting our methods to account for these factors as described in SI Section 2, and chose not to as we estimated that they have only a ~1% effect on the magnitude of sample values in our study regions, and are therefore not significant for the purposes of this analysis.

2.2.2. Stationary peak demand model

For the stationary model, we used linear regression to relate peak demand in balancing authorities to T_{max}. We used the range T_{max} = 25 °C to 40 °C (77 °F to 104 °F), as was common convention in similar studies [11,47], and the nineteen studies of climate effects on power demand summarized in [14], to fit the model parameters. We then scaled the model by the fraction of residential and commercial buildings in the balancing authority [48] to the county [49,50]. Stationary approaches are inherently biased by unavoidable factors, including the observation range and choice in sample range, in our case $T_{max} \geq 25$ °C. AC units are generally sized for buildings based on historical weather patterns, so it is coincidental that the aggregate historical performance fits well to a straight line. We excluded all observations less than 25 °C to avoid capturing increase in loads at colder temperatures due to the use of electric heating appliances; had we not excluded these observations, peak demand would have visually appeared "U-shaped" when plotted over T_{max}, and an "x^2" type of function could have had a high correlation. Such a function would have produced significantly higher estimates of peak demand at higher air temperatures than a linear function.

2.2.3. Non-stationary model

For the non-stationary approach, we created a structural equation model based on knowledge of the relevant infrastructure and their thermal and electrical performance characteristics, then fit that SEM to the observed data. The most significant temperature-dependent electrical loads in the study regions were AC units, and we chose to model the change in peak demand as characteristic of changes in AC performance only, as explained in SI Sections 3 and 4. We modeled all AC units as split indoor-outdoor dry air-cooled engineering designs based on previous performance characterization studies in [51,52], which showed an increase in active load of 1.33%kW per 1 °C ± 0.35% for seven different AC units. Fig. 2, inspired by [53], provides a visual representation of the micro- and macro-scale system dynamics that we considered as the premise for our SEM. As outdoor thermal forces increase, ambient dry-bulb air temperature (T_{dry}) increases, and individual AC loads increase. Duty cycles increase proportional to the ratio of incoming and outgoing building thermal energy ($\dot{Q}_{in}/\dot{Q}_{out}$) at the thermostat set point. At higher T_{max}, the expected number of ACs simultaneously active in a region during the peak period increases up to a theoretical limit of 100%. The mid-section steepness of the s-curve is characteristic of the observed behavior of AC units within a region. We used the corresponding peak demand observations to fit the SEM. Limitations of this stochastic modeling approach are in its ability to predict usage patterns of individual AC units at lower temperatures. Our primary objective, however, was to gain insight into the right side of the aggregate peak demand tail, where—at unprecedented high air temperatures—AC engagement approaches 100%. Therefore, as discussed in SI Section 4, given the large sample size, we did not consider those methodological limitations prohibitive for this study.

The mathematical form of the SEM is in Eqs. (1)–(3), and the nomenclature in Table 1. Daily peak demand (D_{peak}) is equal to the base peak demand (D_{base}) plus, the product of the macro-scale component, the expected coincident number of ACs in active mode (n), and the micro-scale component, the average AC load (AC_L). Base peak demand was set equal to average peak demand for days where T_{max} was between

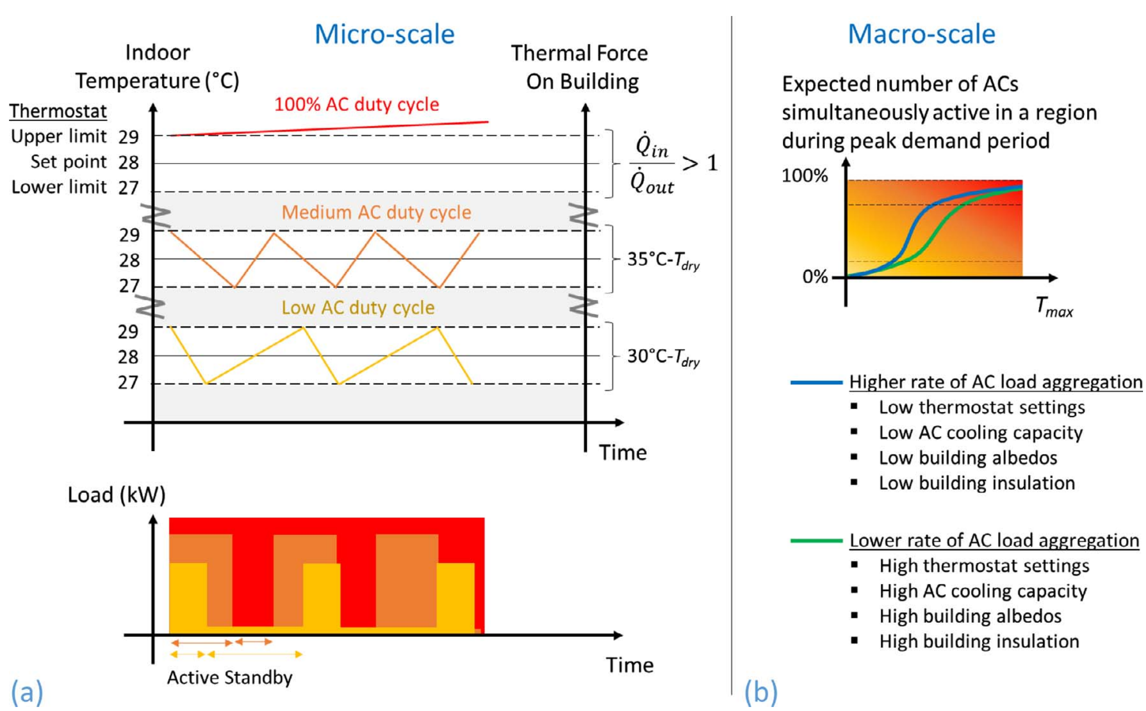

Fig. 2. Outdoor temperature effects on AC operations. (a) Micro-scale. Key performance metrics for a single building, with one standard AC unit, at three different levels of constant thermal force on the building: yellow – low, orange – medium, and red – high. In reality, thermal forces change over time, e.g. hourly, daily, seasonally, and with sunlight, wind, rain, etc. (b) Macro-scale. Cumulative AC activity as a function of T_{max}, and comparison of relative influencing factors at the building level. (For interpretation of the references to colour in this figure legend, the reader is referred to the web version of this article.)

Table 1
SEM nomenclature.

Symbol	Units	Description
Dependent/response variable		
D_{peak}	GW	Daily peak demand in region
Structurally interdependent variables		
n	# ACs	Number of ACs coincidently active during peak demand
AC_L	kW	Average load of one AC unit while in active mode
Independent predictor variables		
T_{max}	°C	Daily maximum ambient air temperature (dry bulb temperature)
D_{base}	GW	Base daily peak demand in region, equal to the average demand between T_{max} = 22–24 °C (72 ~ 75 °F)
Q_{AC}	# ACs	Quantity of ACs in region
Constants		
AC_{LF}	%/°C	AC load increase factor (= 1.33%kW/1 °C)
T_{NL}	°C	Nominal load temperature, T_{max} value for AC_{NL} (= 29 °C, 85 °F)
e	–	Euler's number (= 2.7182…)
Model fit parameters		
AC_{CR}	Ln(# ACs)/ 1 °C-T_{max}	AC coincident rate, log of coincident AC duty cycles during the peak demand period. Represents the steepness of the s-curve
AC_{NL}	kW	Average AC nominal load while in active mode. Represents average AC size in terms of electrical load at baseline temperature T_{NL}

22 °C and 24 °C (72–75 °F) to serve as a sample independent of electric cooling or heating. To estimate the number of ACs simultaneously running at a particular T_{max}, equation (2), we formulated a logistic model (s-curve) to range from one (statistically equal to zero in this case) to the total number of ACs in the system (Q_{AC}) as is an appropriate formulation for such "non-linear chaotic" system behaviors [54]. The total number of ACs is estimated to be the sum of residential and commercial customers listed for each balancing authority in EIA form 861 [48], weighted by the average percentage of central ACs installed in residences for Maricopa and Los Angeles (95% and 48%) per county assessor records as reported in [50]. The log-rate of coincident AC duty cycles during peak demand (AC_{CR}) was fit to the data and represents the steepness of the curve. We defined the population average AC load (AC_L) in equation (3), as a geometric function equal to the average nominal load (AC_{NL}) that is also fit to the data, times the compound load factor (AC_{LF}) relative to the nominal load temperature (T_{NL}).

$$D_{peak} = D_{base} + n{\cdot}AC_L{\cdot}10^{-6} \quad (GW) \tag{1}$$

$$n = \frac{1}{Q_{AC}^{-1} + e^{-AC_{CR}\cdot T_{max}}} \quad (\#ACs) \tag{2}$$

$$AC_L = AC_{NL}{\cdot}[(1 + AC_{LF})^{(T_{max}-T_{NL})}] \quad (kW/1AC) \tag{3}$$

To model peak demand for the two counties, we fit and then scaled the SEM. We optimized the AC_{CR} and AC_{NL} parameters to minimize the root mean squared error of the residuals for the balancing authorities' peak demand at $T_{max} \geq 25$ °C. Observations below 25 °C were explicitly out of scope of the fitting procedure, as the model's purpose is not to explain the effect of colder weather on peak demand due to electric heating. We defined the best-fit model as the model with the highest R^2-value from this approach. Regression results for all balancing authority and weather station combinations are included in SI Section 5. County peak demand was estimated by allocating the balancing authority demand to the quantity of residential and commercial customers by annual energy consumption (% Wh) [48], and scaling up by the total number of residential and commercial buildings in each county per [50]. We assumed the same level of AC penetration in the balancing authorities as the central-AC installation rate in respective counties per [49,50]. We considered model sensitivity to AC penetration, and characterized the effects of additional undocumented non-central ACs (e.g. window ACs or large wet-cooled commercial ACs) in the system on model results in SI Section 6. We did not differentiate between residential and commercial buildings for average unit load (AC_L), nominal load (AC_{NL}), or load increase factor (AC_{LF}). The most significant uncertainty factors included in upper- and lower-prediction ranges were *T90* values, as shown in Fig. 1b, unit load increase factor (AC_{LF}) as previously described, and the range of the base peak demand (D_{base}). We parameterized and scaled the range of the base peak demand (D_{base}), as the range of peak demand samples collected for each balancing authority for T_{max} ranging from 22 °C to 24 °C. We attribute this range to coincident econometric factors and intrinsic heteroscedasticity.

2.3. Generation capacity

We modeled generation capacity as a constant for the stationary paradigm to go with the straight-line approach for peak demand, and as a linear function of T_{max} for the non-stationary paradigm and our structural equation model of peak demand. The 2014 EIA form 860 lists US power generators by geographic location, and we used the summertime generation capacity values for hydroelectric, natural gas (NG), nuclear, and solar PV generation types in Maricopa and Los Angeles counties respectively [55]. We used those values as-is for the stationary approach, and as values for T_{max} at respective *T90s* in the non-stationary approach. Generation values listed in these counties did not include energy efficiency, demand response, or distributed energy resources—all of which are considered at some level in resource adequacy planning [12]–nor coal, wind, oil, wood, landfill gas, pumped storage, hydropower, or transmission imports which also provide power within the states of Arizona and California [55]. Likewise, Maricopa and Los Angeles counties did not have any open-loop cooled plants and therefore we did not consider the performance of such plant types. The counties had relatively small amounts of conventional hydropower and solar PV resources within their geographic boundaries; explanation of approaches to their non-stationary parameter values during unprecedented heat waves are in SI Section 6. The significant generation resources in the study regions were nuclear and NG plants, both of which rely on thermal processes that are sensitive to temperature.

As explained in SI Section 6, nuclear and natural gas power plants are large, complex, and actively managed engineered systems with widely varying technologies and operator practices that affect performance [56]. Since it is not feasible to accurately model each plant's operational details in this study, we chose to parameterize a range of values for derating factors as a linear percent per 1 °C-T_{max} using a range of results from previous empirical studies of plant performance, including dry-cooled plants (0.5–0.65% [57], 0.83% [1], 0.7–1% [47]), combined-cycle natural gas (CCNG) (0.2–0.4% [58]), and wet-cooled plants (0% plant efficiency as a predictor of capacity in [59]). We allocated CCNG plants as 1/3 dry and 2/3 wet, as that was the approximate ratio listed in EIA form 860 per code reporting: CA – combined cycle steam part, CS – combined cycle single shaft, and CT – combustion turbine. We set the base value of NG dry at 0.6% such that the CCNG allocation would be in the observation range; CCNG accounted for 88% and 62% of NG capacity in Maricopa and Los Angeles respectively.

2.4. Local reserve margin

To model LRMs for unprecedented high temperatures, and compare stationary and non-stationary paradigms, we combined the output of the respective peak demand and generation capacity models and plotted the resulting LRM curves over a range of daily high temperatures. We calculated LRMs in both absolute (GW) and percentage terms as the amount of generation capacity that exceeds the peak demand for any T_{max}. Planning guidelines for operating reserve margins commonly follow the rule of thumb of ≥15%, and emergency load curtailment orders are issued when that margin falls to less than 5%, [2,27,60,61].

Therefore, we noted T_{max} and LRM at *T90* peak demand, +10%, and +15% as potentially hazardous conditions depending on transmission import capabilities. We then compared those values to our modeled margins at historic and projected air temperatures, and considered the additional need for local generation or power imports in Los Angeles and reduced capability for power exports from Phoenix.

3. Results

3.1. Air temperatures

The stationary approaches to parameterize *T90* resulted in values that were inconsistently lower than historical and projected T_{max}. As shown in Fig. 1b, only one location had *T90*s that were consistently lower than all historical T_{max} in the sample periods, whereas all other locations had some years when a *T90* was higher than another's T_{max}. The ranges of temperatures varied more within Los Angeles than the Phoenix area between the lowest historical *T90* and the highest historical and projected T_{max} (17 °C and 24 °C in Los Angeles vs 6 °C and 15 °C in Maricopa). The larger range in Los Angeles was due to more variable climate from the coastal areas to inland as shown in Fig. 1a. The smaller ranges in Maricopa were because the typical summertime climate (sunny, hot, dry, flat, low-wind, urban desert) is relatively closer to the most extreme conditions [37,62]. If the distributions of T_{max} were stationary from year to year, then *T90* would be a reliable statistic to use as an input for risk management purposes, but T_{max} distributions are significantly inconsistent. Using stationary *T90* statistics as inputs in planning processes introduces anti-conservative bias to the 15% safety margin for peak demand.

GCM projections provided ranges of non-stationary future T_{max} values that were higher than historical T_{max} values at most locations. General trends within counties were similar to historical, except that Tarzana, which had the highest average *T90*, only had the third highest projected T_{max}, and East-Burbank, which had the third highest historical T_{max}, had the highest projected future T_{max}. Even a recent sixteen-year historical sample is not sufficient to overcome stationarity bias. Top GCM projections were on average 2 °C higher for end-of-century projections than mid-century, and 1 °C higher for RCP 8.5 than RCP 4.5. The usefulness of the GCM projections was not to predict individual daily temperatures or warming trends, but rather to identify the potential magnitude of heat waves for an upper-boundary on temperature inputs in long-term demand forecasting and infrastructure planning processes. Our non-stationary approach estimated a range for the peak temperatures that regions could experience, and those are possible future conditions that should be explicitly considered in planning according to the ISO principles of risk management [63].

3.2. Peak demand

The SEM and straight-line model projections for peak demand significantly overlapped in the historical range of 25–40 °C (77–104 °F), and diverged significantly at the highest GCM projected temperatures. As shown in Fig. 3a, the straight-line model results were that Phoenix and Los Angeles expect peak demands of 12GW and 21GW at the highest projected temperatures, or 28% and 23% higher than for historical T_{max}. The SEM model results were 8–10 GW and 13–19 GW respectively, or 6% and 7% higher than for historical T_{max}.

Total peak demand historically increases more in Phoenix during the summer with increases in air temperatures than in Los Angeles, but results indicate that the effects of non-stationary extreme heat events are greater in Los Angeles than in Phoenix. As shown in Fig. 3a, from 25 °C to local *T90*s, peak demand increased in Phoenix and Los Angeles from 3.5 GW to 7.6 GW and 8.2 GW to 11.7 GW (or by 120% and 40% respectively). Peak demand increased more in Phoenix in its historical range because the region has approximately twice as many ACs and its historical *T90* is 11 °C (20 °F) higher than Los Angeles's. From historical *T90* to the highest projected T_{max} (56 °C and 58 °C or 133 °F and 136 °F) however, peak demand increased more in Los Angeles than Phoenix, another 3.9 GW vs 1.2 GW or 34% vs 16%. The larger marginal increase in peak demand in Los Angeles was due to the larger relative difference between historical *T90* and projected T_{max}, which we note again are inclusive of almost a century's worth of potential heat waves that are much closer in terms of absolute temperatures for the two regions than average or *T90* temperatures. As shown in Fig. 3b, Phoenix's ACs expect to already be running at nearly 100% duty cycle at its historic *T90* of 44 °C (111 °F), whereas Los Angeles's ACs expect to only be running at about 60% duty cycle at its *T90* of 33 °C (91 °F). Thus, the potential for record-breaking heat waves to affect peak demand is more significant in Los Angeles than Phoenix. See SI Section 5 for model parameter details.

3.3. Generation capacity

Generation capacities were held constant in the stationary models, and derated up to 7% in the non-stationary models. Stationary and non-stationary values are listed side-by-side in Table 2 column A under the respective *T90* and projected block maxima temperature values for each county. The derating factors used are listed in column B. Dry natural gas generators—either entire plants and or the combustion engine portion of CCNGs—were the only significant source of generation capacity loss in the model for the two counties. The expected generation capacity reduction between stationary *T90* and non-stationary GCM temperatures was from 3.3 GW and 3.2 GW to 3.0 GW and 2.7 GW in Phoenix and Los Angeles respectively, and potentially another 0.3 GW less in each depending on the cooling technology per SI Section 6. This represents a loss of 9% and 16% of dry natural gas plant capacity, or 2.2% and 4.2% loss of total local generation capacity.

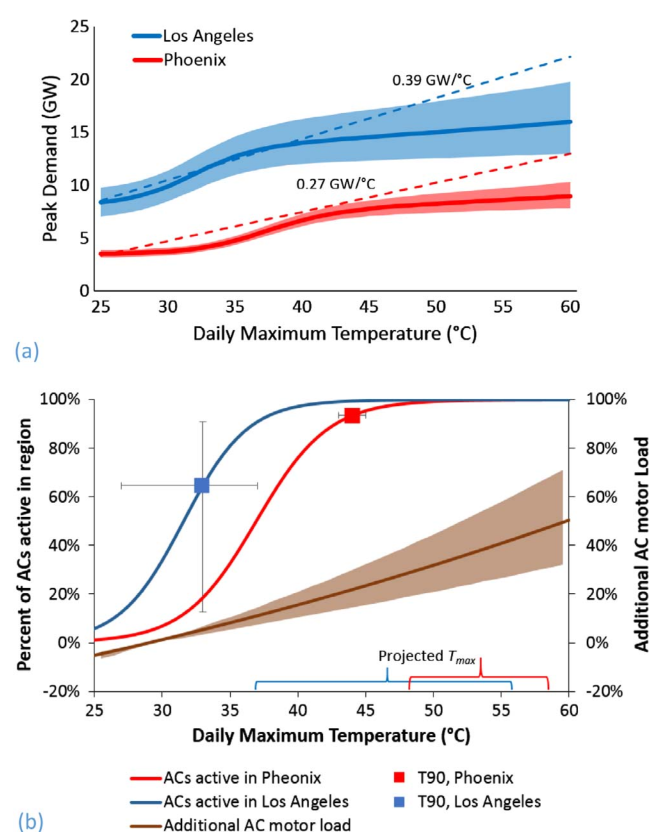

Fig. 3. (a) Peak demand. Solid lines represent SEM approach. Dotted lines represent straight-line approach. (b) Peak demand SEM factors. The two s-curved lines are expected values, equal to Eq. (2) divided by Q_{AC}. *T90* ranges are for the average of the 16 years of values at each of the four locations sampled.

Table 2
Summertime generation capacities and derating factors.

	A – Generation capacity (MW)				B – Derating factor		
	Phoenix		Los Angeles		(%/1 °C-T_{max})		
Generation type / @T_{max}	44 °C	58 °C	33 °C	56 °C	Low	Base	High
Hydroelectric	95	95	341	341	–	–	–
Natural Gas (dry)	3,292	3,016	3,178	2,739	0.5%	0.6%	1%
Natural Gas (wet)	6,180	6,180	7,251	7,251	–	–	–
Nuclear	3,937	3,937	–	–	–	–	–
Solar PV	446	424	449	412	0.1%	0.35%	0.6%
Total							
Maricopa	13,950	13,652			0.12%	0.15%	0.26%
Los Angeles			11,219	10,743	0.15%	0.18%	0.31%

3.4. Local reserve margin

In both the straight-line and SEM approaches, LRM results matched the current reality that Phoenix has sizeable electricity export capabilities, and Los Angeles requires significant imports to meet peak demand. As shown in Fig. 4, both counties expect to be able to meet local demand with local generation capacity up to approximately T_{max} equal to their recent average *T90s*. Phoenix expects 70–100%, 6–7 GW, of surplus local generation at its *T90*, whereas Los Angeles expects to break even 1 °C under its *T90*, ± 15% or ± 2GW. Both approaches project positive LRM for Phoenix for the highest projected T_{max} (58 °C or 136 °F). We noted potentially hazardous operational conditions as a relative decrease in LRM of at least 10% to 15% from *T90* peak demand. The hazardous temperature threshold in the linear model for Los Angeles was at 34–36 °C (93–97 °F), and slightly higher at 36–39 °C (97–102 °F) in the SEM model. At the highest projected temperatures for Los Angeles (56 °C or 133 °F), the linear approach projected hazardous conditions with LRM at −84%, or 9.4GW of demand that current local generators would not be able to meet. The SEM approach also projected hazardous conditions with LRM at −31%, or 5GW of demand above local generation capacity. If we sum the peak demand and generation capacities of both Phoenix and Los Angeles, then the total combined LRM would be negative if T_{max} in Phoenix and Los Angeles simultaneously reached 58 °C & 42 °C (136 °F & 108 °F), 45 °C & 48 °C (113 °F & 118 °F), or 39 °C & 56 °C (102 °F & 133 °F).

4. Uncertainty and validation

Estimating LRM was a multi-step process with uncertainty in parameters, methods, and results in each section of the methods. The SEM is not sensitive to marginal errors in AC penetration or AC types. As we explained in SI Section 7, we estimated Los Angeles has on the order of 100,000 undocumented window AC units (~10% of customers), which we inferred through differences in the model fit parameters AC_{NL} and AC_{CR}. This does not significantly affect results. The most significant uncertainties in results stemmed from the range of the temperature-independent peak demand, which we attribute to econometric factors and inherent randomness. Uncertainty ranges were larger in Los Angeles than Phoenix due to higher variability of air temperatures throughout the region. Finer spatial allocation of demand and T_{max} data could significantly reduce this uncertainty as in [12]. The worst-case scenario results for LRM for Los Angeles were at T_{max} = 56 °C (133 °F) where in the linear and SEM approaches an additional 9.4 GW (84%) and 4.9 GW (31%) capacity was projected necessary to meet demand. The combined effects of uncertainty for the SEM approach at T_{max} = 56 °C and 58 °C were low, medium, and high estimates of LRM of −2.3 GW, −4.9 GW, and −8.2 GW (−31% ± 12%) for Los Angeles and 3.6 GW, 4.8 GW, and 5.7 GW (55% ± 19%) for Phoenix. The SEM results were that T_{max} would be potentially hazardous at temperatures of 36–39 °C (97–102 °F) or higher, which is consistent with the 2014 extreme heat event where T_{max} reached 38 °C (100 °F) in downtown Los Angeles, and the Los Angeles Department of Water and Power alerted customers to curtail power [17,64],. The recent study in [47], used straight-line methods for peak demand and generation capacity to estimate a need for up to 38.5% additional generation capacity for the entire state of California under end-of-century A2 and B1 climate change emissions scenarios. See SI Section 7 for further details of uncertainty and validation.

5. Discussion: long-term strategic planning for climate non-stationarity

Stationarity assumptions had significant effects on forecasts of daily high temperatures, peak demand, generation capacity, and local reserve margins. Updating long-term forecasting processes to consider climate non-stationarity explicitly would enable better evaluation of risks. Without a clear understanding of uncertainties in both climate and power systems, risk managers lack actionable information as to whether operating margins are sufficient to meet tolerances for reliability and security. While our findings indicate value in creating new knowledge of the effects of climate non-stationarity on power systems, creating new knowledge "on paper" is a very different proposition than creating new infrastructure implementations in practice.

There are many ways to maintain reserve margins and reliable power services in grid systems, all of which have various tradeoffs. As shown in Fig. 5, we systematically considered several technology implementations, market incentives, and urban form options that can affect LRMs. We included load variance explicitly because less variance

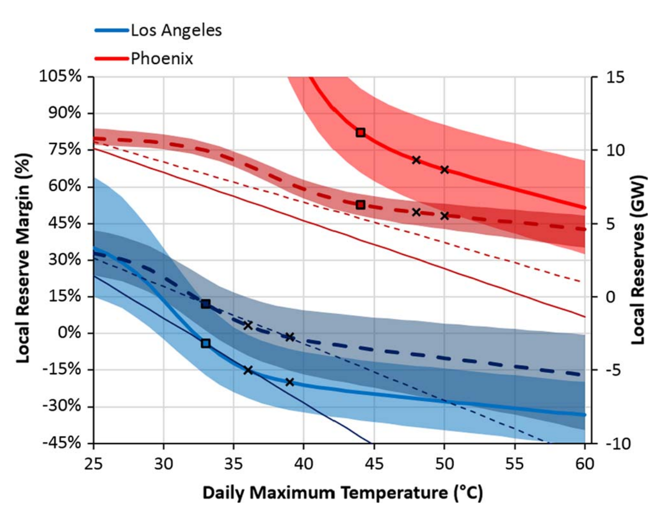

Fig. 4. Model results for daily maximum temperature effects on local bulk power reserves. Thick lines and corresponding shaded areas represent SEM results, and thin lines represent straight-line model averages. Solid lines represent LRMs as a percentage, and dotted lines as GW. Average *T90* values are marked with squares, and relative decreases of 10% and 15% LRM are marked with X's.

	Options / Effects	Resource adequacy: Climate-independent peak load	Resource adequacy: Climate-dependent peak load	Resource adequacy: Bulk gen. & transmission capacity	Resource adequacy: Load variance	Other factors: Total energy consumption	Other factors: Power quality	Other factors: Power congestion	Other factors: Water use	Other factors: Greenhouse gas emissions
Technology implementation										
Resources	Distributed solar PV without VAR control	↓	↓	-	↓	-	⇩	↓	-	-
Resources	Distributed solar PV with smart-inverter & energy storage	↓	↓	-	↓	-	↑	↓	-	-
Resources	Combined cycle natural gas plant	-	-	↑	-	-	↑	⇧	⇧	⇧
Resources	Nuclear power plant	-	-	↑	-	-	↑	⇧	⇧	-
Loads	General appliances: higher energy efficiency standards	↓	↓	-	↓	↓	-	↓	-	↓
Loads	ACs: variable speed motors for refrigerant systems	-	-	-	-	-	↑	-	-	-
Loads	ACs: dual-systems with ice thermal storage	-	↓	-	↓	-	-	↓	⇧	-
Loads	ACs: water-based evaporative systems	-	↓	-	↓	↓	↑	↓	⇧	↓
Market incentives										
Util.	Utility profits dependent on energy sales	⇧	⇧	-	⇧	⇧	-	⇧	-	⇧
Util.	Utility profits dependent on load consistency	↓	↓	-	↓	↓	-	↓	-	↓
Ratepayer	Time-of-use rates with summertime super-peak	↓	↓	-	↓	-	-	↓	-	-
Ratepayer	Demand response incentives	↓	↓	-	↓	-	-	↓	-	⇧
Ratepayer	Economically viable pro-sumer options	↓	↓	-	↓	-	-	↓	-	↓
Ratepayer	Energy efficiency rebates	↓	↓	-	↓	↓	-	↓	-	↓
Urban form										
	High-density transit oriented development	↓	↓	-	↓	↓	-	-	↓	↓
	High building albedo and shading	↓	↓	-	↓	↓	-	↓	-	↓
	High building thermal insulation	↓	↓	-	↓	↓	-	↓	-	↓

Fig. 5. Climate risk mitigation options and effects. Arrows indicate an increase or decrease in the factor. Solid green indicates higher efficiencies and or conservation of limited natural resources. Hollow red indicates the opposite.

means more consistent load, more capacity for contingencies, and lower operations and maintenance costs [3]. We also identified effects of those options on several other complex interdependent factors that are priorities for stakeholders. The remainder of this discussion section follows the structure of the options listed in Fig. 5 that can mitigate the risk of LRM shortages in the event of unprecedented heat waves. We do not intend for this discussion to be exhaustive nor advocate any particular option; our intention is to advance the discourse of this complex topic in a clear and structured manner.

5.1. Technology implementation – electricity supply resources

Additional electricity supply resources will be required to meet demand as population growth, urban development, and technology electrification continues. New resources will likely include distributed energy resources (DERs), natural gas generation, and nuclear technologies [5,35]. Most solar PV, storage and demand response systems in the US Southwest are installed “behind-the-meter” [65]. In these cases, solar PV provides an average decrease in net load [66], and circumstantially affects peak loads [67]. When solar PV is combined with storage, demand response, and advanced inverter controls, then the combined set of assets can yield higher load factors and offer ancillary services necessary to maintain power quality [68–70]. Because of this, DERs may one day offset the need a significant portion of bulk generation systems and delivery infrastructure in the US. CCNG plants are a bulk generation solution expected to meet a large portion of future peak loads [5]. They are relatively low-cost and agile resources capable of short turn-on times with fast ramping rates to meet demand spikes, but do not have any effect on load variance, require transmission systems, use water resources, and emit greenhouse gases [71]. Nuclear plants produce energy at a very low price, but that energy is used to meet baseload demand only [5]. Nuclear technology also currently consumes significant quantities of fresh water or grey water for cooling operations [72]. While nuclear plants operate without greenhouse gas emissions, non-stationary climate events have resulted in radioactive containment failures such as the incident at Fukushima [73].

5.2. Technology implementation – building cooling load

More efficient appliances provide the same functionality with less energy consumption. If appliances are more efficient, then peak load is reduced, and the system is less vulnerable to inaccurate estimations of demand. Likewise, total energy consumption is reduced and greenhouse gas emissions per appliance are reduced as well. AC units in the US are currently rated for efficiency and sold primarily on the basis of SEER metrics that are based on performance over a range of moderately warm to hot temperatures. EER ratings are a better indicator of performance efficiency during heat wave conditions however [74], and it is possible to design AC units that consume less power during the hottest conditions. Variable speed motors can improve power quality by reducing AC cycling, but whether or not they have a significant effect on peak load depends on the application [75]. AC systems with thermal storage can significantly offset peak load, but add cost [52,76]. Water-based evaporative systems use much less power in general, but require water to operate, and are often not accepted by users as the sole-source of air conditioning due to insufficient comfort levels when the weather is both hot and humid [62,77].

5.3. Market incentives – supply side & utilities

Some studies suggest that the traditional utility business model, that couples energy sales to profits, is not compatible with certain energy efficiency goals or large amounts of distributed energy resources [78]. The former issue occurs when utility revenues are primarily dependent on total energy sales, but the costs of providing reliable infrastructure are primarily dependent on capital expenditures, operations, and maintenance [78]. Profits increase with volumetric energy sales, and costs are relatively flat. Therefore, financial incentives must exist to be relatively inefficient in some processes. Hence, public regulatory commissions exist to oversee the prices set for ratepayers. The alternative business model is referred to as a "decoupled" market, where "excess" profits are carried forward and accounted for in adjusting the following years' prices [79,80]. When utility profits are decoupled from energy sales, load serving entities can implement effective conservation programs without violating fiduciary responsibility to owners [81]. This structure has been implemented in several states with positive effects on energy efficiency. For example, California's per-capita annual energy consumption has remained relatively flat since decoupling was implemented in the 1980s, whereas many other states' has steadily risen [82]. Market design determines rules by which participants do business and trade [83]. If utilities' profits were a function of key reliability precursors, such as smaller load variance, then utilities would have a direct incentive to reduce peak load (including shifting it to off-peak hours), resulting in less congestion, higher utilization of lower-cost base-load bulk generation resources, and more contingency capacity for future record-breaking heat events.

5.4. Market incentives – demand side & ratepayers

One philosophy for evaluating public policy is to consider whether the rules are equitable, efficient, transparent, administratively simple, and support achieving greater policy goals [84]. Current retail electricity rate schedules in Los Angeles and Phoenix generally meet these criteria via monthly energy billing with tiered and time of use rates [85–88]. Charging residential ratepayers monthly based on total energy use is simple, transparent, equitable, and promotes energy efficiency. Higher electricity prices for more consumption and during peak hours reduces peak load by incentivizing ratepayers to use less energy and to shift flexible or non-critical usage to off-peak hours when electricity can be generated at lower cost [89]. Incentivizing ratepayers to turn off loads in the form of demand response relieves congestion on the grid; however, the majority of that relief comes from industrial customers who often switch to onsite diesel power or natural gas combined heat and power units [90]. Rebates are available in some localities for ratepayers to obtain solar PV, storage, or demand management technologies [91]. One-time rebates for building energy efficiency enhancements have also been demonstrated effective at reducing demand and peak load [92]. Overall, these incentives generally reflect the philosophy that electricity is both a critical infrastructure necessity and a non-critical commodity. Electricity is critical for powering infrastructure systems such as water, transportation, food, fuel, communications, and finance [93]. It is also critical in residential buildings for lighting, cooking, cleaning, and air temperature control.

5.5. Urban form

Per capita power demand and energy consumption are both significantly lower in high density, multi-unit housing structures than in lower-density, single-dwelling unit buildings [94]. Multi-unit buildings benefit from shared wall space, and in larger cases often centralized industrial air conditioning systems that are more efficient and less sensitive to weather [52]. Regardless of building type, high albedo (e.g. white roofs), shade (e.g. trees on the west side), and better thermal insulation in general, significantly improves building energy efficiencies [95] and reduces peak load and load variance.

5.6. Summary

Investments that reduce peak load and load variance per capita mitigate the hazard potential of record-breaking heat waves. Application of risk management principles and free-market incentives are generally effective; however, with limited options and systemic values that are not directly monetized, some regulations are necessary to provide minimum standards where there otherwise might not be any. Because electric power infrastructure systems are so large, complex, and interdependent within and across other systems, myopic "one-size fits all" techno-centric solutions to climate hazards are unlikely to have significant impact. Climate hazards can be reasonably mitigated by considering multiple options from multiple stakeholders' perspectives and accordingly investing in a portfolio of options.

6. Conclusions

Planning and operating power infrastructure based on stationary climate assumptions exposes the system to measurable and avoidable risks. Insufficient planning for climate non-stationarity will result in low reserve margins during record-breaking heat waves, higher probability of infrastructure failures, and system vulnerability to multiple outages including security threats disabling entire cities' critical infrastructure. Linear correlation methods result in overestimation of the effects heat waves on LRM, and could result in wasteful expenditures to maintain safety margins if used in investment planning processes. Our SEM approach is a more reasonable estimation method. As new knowledge enables better understanding of the climate, new methods for managing risks of low-probability high-impact events are valuable to maintaining reliable electricity infrastructure systems. Future work should consider additional climate non-stationarity factors, including probability of simultaneous heat waves across nearby geographies [25–27], wildfire potential [96,47], drought [1,97], and transmission import capabilities from neighboring regions, as well as relevant changing physical, network, and sociotechnical attributes of aging delivery systems and building loads [13,47,98]. Strategic actions can be taken to reduce the risk of LRM shortages from non-stationary heat events without compromising other stakeholder objectives, including implementing technology, market incentives, and urban forms that reduce peak load and load variance per capita.

Acknowledgments

This material is based in part upon work supported by the National Science Foundation under grant number 1360509, 2014-2017, Advancing Infrastructure and Institutional Resilience to Climate Change for Coupled Water-Energy Systems, and the California Energy Commission under grant number CEC EPC-15-007, Climate Change in Los Angeles County: Grid Vulnerability to Extreme Events. Any opinions, findings, and conclusions or recommendations expressed in this material are those of the authors and do not necessarily reflect the views of the National Science Foundation or the California Energy Commission.

A. Supplementary data

Supplementary data associated with this article can be found, in the online version, at http://dx.doi.org/10.1016/j.apenergy.2017.08.141.

References

[1] Bartos MD, Chester MV. Impacts of climate change on electric power supply in the Western United States. Nat Clim Chang 2015;5(8):748–52.
[2] NERC, 2015 Long-Term Reliability Assessment; 2015.
[3] Willis HL, Welch GV, Schrieber RR. Aging power delivery infrastructures. Marcel Dekker, Inc.; 2001.
[4] Ralff-Douglas K. Climate adaptation in the electric sector: vulnerability assessments & resiliency plans; 2016.
[5] APS. APS 2014 Integrated resource plan; 2014.
[6] WECC. Loads and resources methods and assumptions. Salt Lake City, Utah; 2014.
[7] SRP. SRP integrated resource plan FY; 2013.
[8] Kyselý J, Picek J, Beranová R. Estimating extremes in climate change simulations using the peaks-over-threshold method with a non-stationary threshold. Glob Planet Change 2010;72(1–2):55–68.
[9] Hall A, Sun F, Walton D, Capps S, Qu X, Huang H-Y, Berg N, Jousse A, Schwartz M,

Nakamura M, Cerezo-Mota R. Mid-century warming in the Los Angeles Region 2012; 1(33).
[10] Miller NL, Jin J, Hayhoe K, Auffhammer M. Climate change, extreme heat, and electricity demand in California. CEC-500-2007-023; 2007.
[11] Sathaye JA, Dale LL, Larsen PH, Fitts GA, Koy K, Lewis SM, de Lucena AFP. Estimating impacts of warming temperatures on California's electricity system. Glob Environ Chang 2013;23(2):499–511.
[12] Garcia-cerrutti M, Junker B, Bender S, Jones M. Revised short-term (2011–2012) peak demand forecast commission. Energy 2012.
[13] Bartos M, Chester M, Johnson N, Gorman B, Eisenberg D, Linkov I, Bates M. Impacts of rising air temperatures on electric transmission ampacity and peak electricity load in the United States. Environ Res Lett 2016.
[14] Santamouris M, Cartalis C, Synnefa A, Kolokotsa D. On the impact of urban heat island and global warming on the power demand and electricity consumption of buildings—a review. Energy Build 2015;98:119–24.
[15] Sailor DJ, Muñoz JR. Sensitivity of electricity and natural gas consumption to climate in the USA – methodology and results for eight states. Energy 1997;22(10):987–98.
[16] Sailor DJ. Relating residential and commercial sector electricity loads to climate – evaluating state level sensitivities and vulnerabilities. Energy 2001;26(7):645–57.
[17] Barry Fisher. STAT OF THE WEEK: Los Angeles shatters its record for peak electric demand, twice - Opower: Opower; 2014. Available: https://blog.opower.com/2014/09/peak-electric-demand-record-los-angeles/.
[18] Jerod MacDonald-Evoy. Power outages impact thousands around Arizona. The Arizona Republic; 2016. Available: http://www.azcentral.com/story/news/local/mesa-breaking/2016/06/05/1900-mesa-homes-lose-power-record-breaking-heat/85464650/.
[19] NERC. Technical Analysis of the August 14, 2003, Blackout; 2004.
[20] Ferc and Nerc. Arizona-Southern California Outages on September 8 2011; 2012.
[21] Raineri R, Ríos S, Schiele D. Technical and economic aspects of ancillary services markets in the electric power industry: an international comparison. Energy Policy 2006;34(13):1540–55.
[22] Smith R. Assault on California Power Station Raises Alarm on Potential for Terrorism. Wall Str J 2014:1–7.
[23] Salmeron J, Wood K, Baldick R. Analysis of electric grid security under terrorist threat. IEEE Trans Power Syst 2004;19(2):905–12.
[24] Burillo D, Chester M, Ruddell B. Electric grid vulnerabilities to rising air temperatures in Arizona. Procedia Eng 2016;145:1346–53.
[25] WECC. 2014 Power Supply Assessment; 2014.
[26] CPUC. Energy Division Proposal for Proceeding 14-10-010 Order Instituting Rulemaking to Oversee the Resource Adequacy Program, Consider Program Refinements, and Establish Annual Local and Flexible Procurement Obligations for the 2016 and 2017 Compliance Years; 2016.
[27] NERC. Planning Resource Adequacy Analysis, Assessment and Documentation, USA; 2015. p. 8.
[28] SocalEV. SoCal EV - Utility Service Territories; 2015. Available: http://www.socalev.org/aboutus/territories.html [Accessed: 12-Dec-2016].
[29] LADWP. LADWP Service Territory Map. Available: http://www.myladwp.com/ [Accessed: 19-Oct-2016].
[30] APS. APS Service Territory Map; 2016. Available: https://www.aps.com/library/communications1/AZ_Map.pdf [Accessed: 03-Dec-2016].
[31] SRP. SRP Electric Service Area; 2016. Available: http://www.srpnet.com/about/pdfx/ElectricServiceAreaMap.pdf [Accessed: 03-Dec-2016].
[32] Pfeifenberger J. Transmission planning: economic vs. reliability projects; 2010.
[33] NERC. CIP-014-1 – Physical security; 2015.
[34] US Census Bureau 2010 Census Interactive Population Map. Available: https://www.census.gov/2010census/popmap/ [Accessed: 14-Jun-2017].
[35] LADWP. Power Integrated Resource Plan; 2016.
[36] Bowen NK, Guo S. Structural Equation Modeling. Oxford University Press; 2011.
[37] Weather Underground. Historical Weather; 2016. Available: https://www.wunderground.com/history/ [Accessed: 07-Jul-2016].
[38] Brekke L, Thrasher BL, Maurer EP, Pruitt T. Downscaled CMIP3 and CMIP5 Climate Projections, May 2013. p. 1–47.
[39] Google Earth Engine: A Planetary-scale Platform for Environmental Data & Analysis; 2012. Available: https://earthengine.google.org/ [Accessed: 01-May-2015].
[40] Google Earth Engine: GRIDMET; 2012. Available: https://earthengine.google.org/#detail/IDAHO_EPSCOR%2FGRIDMET. [Accessed: 01-Jun-2015].
[41] Abatzoglou JT. Development of gridded surface meteorological data for ecological applications and modelling. Int J Climatol 2013;33(1):121–31.
[42] Zhang X, Zwiers FW, Li G. Monte Carlo experiments on the detection of trends in extreme values. J Clim 2004;17(10):1945–52.
[43] EIA. U.S. Electric System Operating Data – Hourly; 2016. Available: http://www.eia.gov/beta/realtime_grid/#/data/graphs?end=20160916T00&start=20160909T00.
[44] SCE Dynamic Load Profiles; 2016. Available: https://www.sce.com/wps/portal/home/regulatory/load-profiles/dynamic-load-profiles/.
[45] Nahlik MJ, Chester MV, Pincetl SS, Eisenman D, Sivaraman D, English P. Building thermal performance, extreme heat, and climate change. Am Soc Civ Eng 2016.
[46] CEC. Residential Appliance Saturation Study; 2009. Available: http://www.energy.ca.gov/appliances/rass/. [Accessed: 01-Oct-2016].
[47] Sathaye J, Dale L, Larsen P, Fitts G, Koy K, Lewis S, Lucena A. Estimating risk to california energy infrastructure from projected climate change. Publication number: CEC-500-2012-057; 2012.
[48] EIA. Electric power sales, revenue, and energy efficiency Form EIA-861 detailed data files; 2014. Available: https://www.eia.gov/electricity/data/eia861/.
[49] Reyna JL, Chester MV. The growth of urban building stock: unintended lock-in and embedded environmental effects. J Ind Ecol 2015;19(4):524–37.
[50] Fraser AM, Chester MV, Eisenman D, Hondula DM, Pincetl SS, English P, Bondank E. Household accessibility to heat refuges: residential air conditioning, public cooled space, and walkability. Environ. Plan. B Plan. Des. 2016.
[51] Faramarzi R, Coburn B, Sarhadian R, Mitchell S, Pierce RA. Performance evaluation of rooftop air conditioning units at high ambient temperatures; 2004.
[52] Bush J, Ruddell B. Field testing an ice storage air conditioner in Phoenix, Arizona, EPRI, September 2015.
[53] Lu N. An evaluation of the HVAC load potential for providing load balancing service. IEEE Trans Smart Grid 2012;3(3):1263–70.
[54] Strogatz SH. Nonlinear dynamics and Chaos. Second Edi: Westview Press; 2015.
[55] EIA. 2014 Annual Electric Generator data - EIA-860 data file; 2014. Available: https://www.eia.gov/electricity/data/eia860/. [Accessed: 02-Mar-2016].
[56] Hensley JC. Cooling tower fundamentals, second ed.; 2011.
[57] Brooks FJ. GE gas turbine performance characteristics.
[58] Maulbetsch JS, DiFilippo MN. Cost and value of water use at combined-cycle power plants; 2006.
[59] Henry CL, Pratson LF. Effects of environmental temperature change on the efficiency of coal- and natural gas-fired power plants. Environ Sci Technol 2016.
[60] NERC. Planning Reserve Margin; 2016. Available: http://www.nerc.com/pa/RAPA/ri/Pages/PlanningReserveMargin.aspx. [Accessed: 07-Jan-2016].
[61] CEC. High temperatures & electricity demand: an assessment of supply adequacy in California, Trends & Outlook; 1999.
[62] Kumar S, Mathur J, Mathur S, Singh MK, Loftness V. An adaptive approach to define thermal comfort zones on psychrometric chart for naturally ventilated buildings in composite climate of India. Build Environ 2016;109:135–53.
[63] Purdy G. ISO 31000:2009 - Setting a new standard for risk management: Perspective. Risk Anal 2010;30(6):881–6.
[64] LADWP. LADWP customers set all-time record for energy demand of 6,196 Megawatts; 2014. Available: http://www.ladwpnews.com/go/doc/1475/2243054/. [Accessed: 21-Dec-2016].
[65] Andersen G. Net metering and demand charges: state solar policy trends; 2016.
[66] Poullikkas A. A comparative assessment of net metering and feed in tariff schemes for residential PV systems. Sustain Energy Technol Assess 2013;3:1–8.
[67] Janko SA, Arnold MR, Johnson NG. Implications of high-penetration renewables for ratepayers and utilities in the residential solar photovoltaic (PV) market. Appl Energy 2016;180:37–51.
[68] Beach T, Kozinda A, Rao V. Advanced inverters for distributed PV: Latent Opportunities for Loaclized Reactive Power Compensation; 2013.
[69] Armendáriz M, Heleno M, Cardoso G, Mashayekh S, Stadler M, Nordström L. Coordinated microgrid investment and planning process considering the system operator. Appl Energy 2017;200:132–40.
[70] Heydarian-Forushani E, Golshan MEH, Siano P. Evaluating the benefits of coordinated emerging flexible resources in electricity markets. Appl Energy 2017;199:142–54.
[71] Adibhatla S, Kaushik SC. Energy, exergy and economic (3E) analysis of integrated solar direct steam generation combined cycle power plant. Sustain Energy Technol Assess 2017;20:88–97.
[72] Macknick J, Newmark R, Heath G, Hallett KC. Operational water consumption and withdrawal factors for electricity generating technologies: a review of existing literature; 2012.
[73] Asian Development Bank. Climate risk and adaptation in the electric power sector; 2012.
[74] SCE. EER & SEER as predictors of seasonal cooling performance; 2003.
[75] (NEMA) National Electrical Manufacturers Association. Application guide for AC adjustable speed drive systems. IEEE; 2001. p. 73–82.
[76] Ruddell BL, Salamanca F, Mahalov A. Reducing a semiarid city's peak electrical demand using distributed cold thermal energy storage. Appl Energy 2014;134:35–44.
[77] Parsons K. Human thermal environments - the effects of hot, moderate, and cold environments on human health, comfort and performance, 2nd ed. Taylor and Francis; 2003.
[78] Grabel MH. Utility rate cases: the insider's perspective; 2016. p. 1–14.
[79] CPUC, California's Next Step Decoupling 'Plus'. Available: http://www.fishnick.com/pge/Decoupling_Explained.pdf. [Accessed: 20-Oct-2016].
[80] PG & E. How PG & E Makes Money. Available: https://www.pge.com/en_US/residential/rate-plans/how-rates-work/learn-how-rates-are-set/how-pge-makes-money/how-pge-makes-money.page?. [Accessed: 21-Oct-2016].
[81] Bhatti M. From consumers to prosumers: housing for a sustainable future. Hous Stud 1993;8(2):98–108.
[82] Wang D. California Is Proof That Energy Efficiency Works | Greentech Media. Green Tech Media; 2013. Available: https://www.greentechmedia.com/articles/read/California-Is-Proof-That-Energy-Efficiency-Works. [Accessed: 21-Oct-2016].
[83] Brijs T, De Jonghe C, Hobbs BF, Belmans R. Interactions between the design of short-term electricity markets in the CWE region and power system flexibility. Appl Energy 2017;195:36–51.
[84] Lave LB. Improving the management of environmental health. Env Heal Perspect 1985;62:359–63.
[85] APS. Residential rate plans. Available: https://www.aps.com/en/ourcompany/ratesregulationsresources/serviceplaninformation/Pages/residential-sheets.aspx. [Accessed: 15-Mar-2017].
[86] SRP. Residential price plans. Available: https://www.srpnet.com/menu/electricres/priceplans.aspx. [Accessed: 15-Mar-2017].
[87] LADWP. Electric rate schedules. Available: https://ladwp.com/ladwp/faces/ladwp/aboutus/a-financesandreports/a-fr-electricrates/a-fr-er-electricrateschedules;jsessionid=

v7vPYKqTKr3hMPFJps1Y8hGyTXvcLLmKQyhK3L2MMbJNgRQJ5Kh-y!545368516?_adf.ctrl-state=cs0kc1rp1_4&_afrLoop=268583008846984&_afrWindowMode. [Accessed: 15-Mar-2017].

[88] SCE. Residential Rates|Rates & Pricing Choices|SCE Tariff Books|Regulatory Information|Home – SCE. Available: https://www.sce.com/wps/portal/home/regulatory/tariff-books/rates-pricing-choices/residential-rates/!ut/p/b1/tVJNU8IwEP01PYYsbemHtw44WBxUBEbaC5OGtI22SUmDqL_ewHDQEUQO5pRs3r7d93Zxihc4FeSVF0RzKUi1e6fechQPou7QteOhPxpA9DDwB_NHr-vedg0gMQA4cSI4l_-EU5xSoRtd4qSlbE. [Accessed: 15-Mar-2017].

[89] Albadi MH, El-Saadany EF. A summary of demand response in electricity markets. Electr Power Syst Res 2008;78(11):1989–96.

[90] Aghaei J, Alizadeh MI. Demand response in smart electricity grids equipped with renewable energy sources: a review. Renew Sustain Energy Rev 2013;18:64–72.

[91] NC Clean Energy Technology Center. Database of State Incentives for Renewables & Efficiency® – DSIRE. Available: http://www.dsireusa.org/. [Accessed: 01-Mar-2017].

[92] Greening LA, Greene DL, Difiglio C. Energy efficiency and consumption – the rebound effect – a survey. Energy Policy 2000;28(6–7):389–401.

[93] Rinaldi SM, Peerenboom JP, Kelly TK. Identifying, understanding, and analyzing critical infrastructure interdependencies. IEEE Control Syst Mag 2001;21(6):11–25.

[94] Chester MV, Nahlik MJ, Fraser AM, Kimball Ma, Garikapati VM. Integrating life-cycle environmental and economic assessment with transportation and land use planning. Environ Sci Technol Nov. 2013;47(21):12020–8.

[95] Smith C, Levermore G. Designing urban spaces and buildings to improve sustainability and quality of life in a warmer world. Energy Policy 2008;36(12):4558–62.

[96] FERC. The August 14 Blackout Compared With Previous Major North American Outages; 2003.

[97] Mann ME, Gleick PH. Climate change and California drought in the 21st century. Proc Natl Acad Sci 2015;112(13):201503667.

[98] Reyna JL. Developing new methods for analyzing urban energy use in buildings/historic turnover, spatial patterns, and future forecasting. Arizona State University; 2016.